Project 23
Analytical Approach for Qualifying Noise from Advanced Operational Procedures

The Pennsylvania State University/The Massachusetts Institute of Technology

Project Lead Investigator

Philip J. Morris
Boeing/AD Welliver Professor of Aerospace Engineering
Department of Aerospace Engineering
The Pennsylvania State University
233C Hammond Building, University Park, PA 16802
814-863-0157
pjm@psu.edu

University Participants

The Pennsylvania State University

- P.I.: Philip J. Morris, Professor of Aerospace Engineering
- FAA Award Number: 13-C-AJFE-PSU-09. Amendment No. 18
- Period of Performance: November 1, 2014 to August 31, 2016

The Massachusetts Institute of Technology

- P.I.: R. John Hansman, Professor of Aerospace Engineering
- FAA Award Number: 13-C-AJFE-MIT-08. Amendment No. 8
- Period of Performance: November 1, 2014 to August 31, 2016
- Combined Tasks:
    1. Continue development of procedures (MIT lead, PSU support)
    2. Identify requirements for aircraft noise performance modeling (MIT)
    3. Apply technique to advanced operational procedures (MIT)
    4. Identify modeling improvements in current tools (MIT, PSU)

Project Funding Level

PSU: FAA: $176,711. In-kind match, Massport: $176,711.

Investigation Team

Philip J. Morris, PI, The Pennsylvania State University; noise source modeling lead
Victor W. Sparrow, co-PI, The Pennsylvania State University, noise metrics lead
Mrunali Botre, Graduate Research Assistant, The Pennsylvania State University, implementation of noise models
R. John Hansman, PI, The Massachusetts Institute of Technology, noise procedures lead
Brian Yutko, Research Engineer, The Massachusetts Institute of Technology, advanced procedures predictions
Luke Jensen, Research Affiliate, The Massachusetts Institute of Technology, flight procedure design and optimization
Jaqueline Thomas, Graduate Research Assistant, The Massachusetts Institute of Technology, Performance and noise analysis
Cal Brooks, Graduate Research Assistant, The Massachusetts Institute of Technology, Performance and noise analysis
Sandro Salgueiro, Graduate Research Assistant, The Massachusetts Institute of Technology, Air traffic management

Morrisa Brenner, Graduate Research Assistant, The Massachusetts Institute of Technology, Aviation community noise

Project Overview

Noise analysis is one important component of environmental evaluation for new flight procedure design. Communities, airports, regulators, and manufacturers must know the noise implications of new operational techniques prior to implementation. Currently, the Aviation Environmental Design Tool (AEDT) is the primary tools used to evaluate new procedures and traffic intensity levels for calculating noise impact footprints near airports. AEDT noise calculations use Noise-Power-Distance (NPD) interpolation to calculate noise using engine data generated through flight test and/or analysis. A functional relationship between engine throttle setting and atmospheric slant distance yields noise estimates for locations on the surface. The frequency spectrum is obtained from a dataset of representative aircraft families at set power levels and aircraft configurations. This procedure results in a simple and computationally tractable noise estimation capability for engine noise sources only. Aerodynamic and procedural noise contributions are not fully incorporated into the model.
This project aims to improve the fidelity, accuracy, and utility of noise analysis techniques for environmental review of advanced operational procedures. Older generations of jet engines produced significantly more noise than current-generation products. The assumption that jet noise dominates aerodynamic sources may have been reasonable in previous environmental impact studies. However, for new advanced approach and departure procedures, aerodynamic noise reduction may contribute strongly to environmental benefits. For example, in a delayed deceleration approach (DDA), deployment of landing gear and high-lift devices can be delayed until later stages in an approach with higher approach speeds, potentially altering total noise [1]. This effect is not captured using current noise-power-distance (NPD) noise calculations. This illustrates a gap in noise analysis capability for advanced operational procedures.

This project involved a collaborative effort involving Penn State University and the Massachusetts Institute of Technology. MIT had responsibility for noise predictions for different advanced approach procedures and Penn State had the responsibility to assess the quality of noise predictions made by existing aircraft noise prediction codes. The final report contains results for both PSU and MIT for consistency and convenience. All the tasks are interconnected so this report covers all tasks without separation.
.

Combined Tasks

Massachusetts Institute of Technology, Penn State University

Objective

Continued review of the physics driving aerodynamic noise generation from advanced procedures (including speed adjustments, thrust adjustments and timing of high-lift device and/or landing gear deployment). The objective of the task is to guide improvements to current noise analysis techniques incorporating aerodynamic effects. This may take the form of enhanced NPD reference data or direct estimation of noise from a physics-based model such as ANOPP.
Calibration of the noise model will be aided by a variety of data sources and analytical techniques. Operational overflight noise data provided by Massport will be used to help calibrate and refine the model. The data will be correlated with high-resolution PDARS radar track records and NOAA weather models to provide a large set of flyover noise events and the corresponding flight conditions. If needed, this calibration method will be supplemented with other noise data (through FAA-AEE, Volpe, and/or aircraft manufacturers).
.

Research Approach

Definition of Advanced Operational Procedures

Operational procedures refer to the manner in which an aircraft is flown or operated in any phase of flight. Precise definition of a procedure includes the latitude, longitude, speed, thrust, altitude, and configuration of an aircraft as a function of time throughout a given phase of flight. Depending on the type of analysis, this definition may be limited to the approach, departure, cruise, or other phases of flight. Advanced operational procedures are those that use modern technology and procedures (infrastructure, avionics, and air traffic control) to control speed, thrust, ground track, and other variables in a

manner that would not be possible in traditional operations. Examples include performance-based navigation (PBN) procedures with required navigation performance (RNP) and precise speed scheduling for efficiency and noise.
The development of advanced flight operations has been driven by several main factors:

- Evolving airport traffic levels and utilization strategies change the environmental impact of air transportation. These changes can impact noise, emissions, air quality, and climate, motivating the exploration of operational mitigations through advanced procedures.
- Airport throughput may be increased based on airspace and procedural design. Adoption of advanced procedures may increase runway and airspace capacity in constrained areas.
- Airlines may achieve economic advantages from advanced operating procedures, including reduced fuel cost and flight times.
- Policy makers can modernize infrastructure through adoption of new technologies in day-to-day operations.

Although advanced operating procedures exist in all phases of flight, the focus of this project is on proposed advanced procedures for arrivals and departures within the terminal area of an airport. Examples include continuous descent arrivals, delayed deceleration approaches, steep approaches, and high-precision performance-based navigation (PBN) approach and departure procedures including Area Navigation (RNAV) and Required Navigation Performance (RNP). These procedures have the possibility to alter the noise footprint near airports relative to current operations due to:

- Changes in aircraft speed profiles on approach or departure, with a corresponding increase or decrease in aerodynamic noise;
- Changes in aircraft thrust profiles due to configuration changes, acceleration schedules, or speed targets, with a corresponding increase or decrease in engine noise;
- Changed aircraft configuration, such as flap settings and landing gear extension, with a corresponding change in aerodynamic noise generation;
- Concentration or dispersal of aircraft operations on set RNP tracks or procedural profiles.
-

Current Noise Evaluation Standard: NPD Approach

The standard analysis technique for the evaluation of new flight procedures, paths, and schedules is the NPD approach. This approach is implemented in AEDT and some third-party noise evaluation software packages. In this method, empirical data is collected for arrival and departure procedures in several aircraft configurations (characterized by flap setting, thrust level, and landing gear configuration). Based on these configurations, noise levels are interpolated as a function of observer distance from the noise source assuming a standard atmosphere and consistent sound energy dissipation with distance. Noise for thrust levels other than those with data available are determined by interpolating between the available arrival and departure thrust levels. The number of NPD curve sets varies by aircraft type within most of these models, generally ranging from 4 to 12 curves (different power settings or configurations) per engine family. Figure 1shows a typical set of NPD curves used in the noise calculation engine of INM and AEDT.

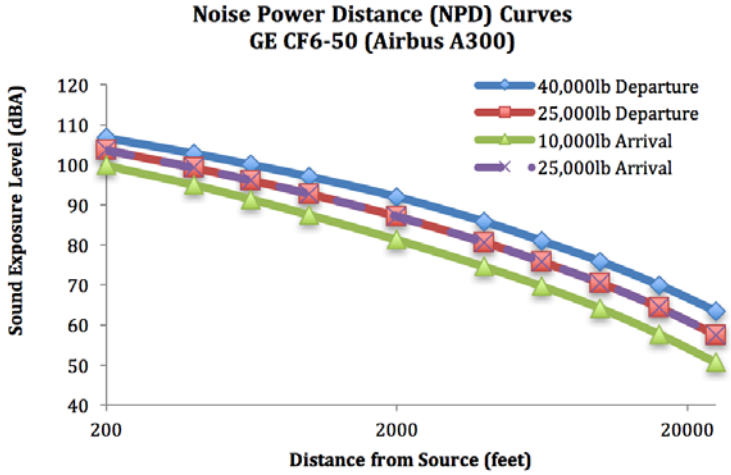

Figure 1. Sample Noise Power Distance (NPD) Curves

The NPD approach allows for noise calculation at a single point on the ground given one flight operation (approach, departure, or overflight). The output of the calculation can be a variety of instantaneous or integrated metrics. The process is then repeated for a full grid of observer locations underlying the flight procedure, allowing for the generation of equal-noise contour lines. Repeating the gridded calculation for a series of flight operations, integrated metrics can be calculated for longer time periods of interest [2]. The resulting contours, such as illustrated in **Error! Reference source not found.**, are an integral part of environmental analyses and mitigation plans for airports. Decisions with respect to residential soundproofing eligibility, land use allocation, and other areas of interest for airport stakeholders rely on noise contours generated analytically and verified empirically [3].

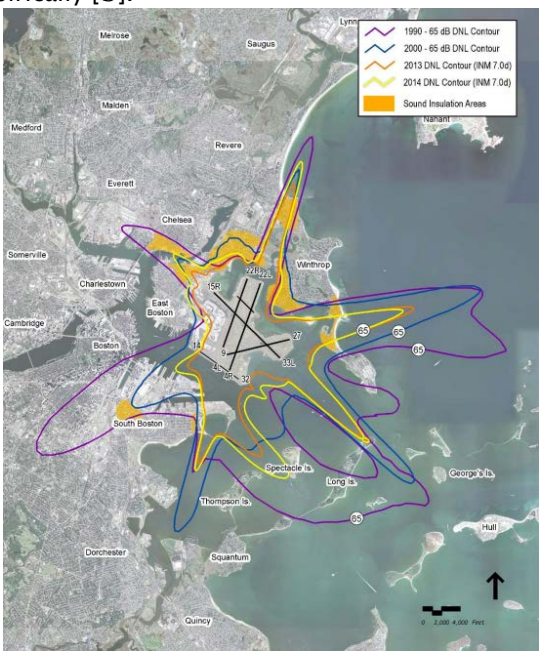

Figure 2. DNL Noise Contours at Boston Logan Airport [4]

While AEDT is an integral component of the environmental regulatory framework, its limited fidelity in aerodynamic noise prevents direct application for the evaluation of advanced operational concepts. Because the NPD approach requires interpolation between a limited set of thrust levels and aircraft configurations, detailed noise changes resulting from aircraft speed or configuration variations cannot be captured. For example, delayed deployment of landing gear and flaps cannot be implemented using standard NPD curve sets, as approach NPD curves assume that the aircraft is in full landing configuration throughout a procedure.

Another limitation of the NPD approach is the limited fidelity of noise shielding and directivity assumptions. The direction of noise propagation from an aircraft depends on the configuration of the aircraft (such as wing and engine geometry), flight attitude (including pitch and bank angle), and the specific source of the noise (i.e. aerodynamic noise from particular structural components or jet mixing noise from the high speed engine exhaust). A detailed treatment of noise in advanced operational procedures requires a higher-fidelity directivity assessment of noise than can be achieved with a simple single-source distance-based noise attenuation model.

One way to address the limitations of the NPD noise calculation method is to evaluate standalone physics-based noise models. Such models should include source modeling, shielding, and propagation. The benefit of such a model is higher fidelity for advanced procedures, although the process does is not directly compatible with existing NPD-based methods. An approach has been developed in proprietary research to convert high-fidelity results into a multi-dimensional lookup table similar to the NPD method but incorporating thrust and configuration variables as well [5]. It is expected that similar methods could be used to incorporate noise characteristics for advanced procedures into existing tool workflows.

High-Fidelity Aircraft Performance and Noise Model Integration

To address the limitations in the NPD-based noise modeling, higher-fidelity physics-based models can be used to capture various noise sources, shielding, and propagation. The outputs of such models can be used to directly calculate noise fields from an overflight or calculate higher-fidelity NPD data sets that better capture aircraft configuration, speed, and thrust levels of interest. The Aircraft Noise Prediction Program (ANOPP) is one model that can be used for this purpose. ANOPP is a NASA developed semi-empirical model that computes noise levels from the airframe and engine components (fan, core, jet, and turbine) at a user-defined observer grid for arbitrary flight procedures[6]. It also accounts for propagation through user-defined atmosphere and aircraft component shielding effects.

ANOPP was originally developed by NASA in the 1970s to provide predictive capabilities in individual aircraft studies and parametric multivariable environmental evaluations. The program was developed with a modular framework and open documentation to allow for interface development with other tools and objectives beyond single-procedure noise analysis. The tool calculates aggregate noise levels from the aircraft engines (fan, core, jet, and turbine noise) and the airframe for a user-defined three-dimensional observer grid. The tool is designed to evaluate noise for a single flight procedure. ANOPP also takes into account noise propagation through a user-defined atmosphere as well as aircraft shielding effects for higher-fidelity directivity analysis.

The methods used in ANOPP for noise computation are semi-empirical, based on historical noise data combined with physical noise models. These models have been improved over time, based on new full-scale and experimental data, but the fundamental noise source models are essentially unchanged. A series of modules take input on aircraft and engine parameters to generate cumulative noise projections for an aircraft configuration and flight procedure. Though ANOPP can provide meaningful noise predictions for conventional tube and wing aircraft configurations, its use for unconventional aircraft or unconventional procedures is challenging.

Aircraft and engine component geometry and performance parameters are also required for advanced procedural noise analysis with ANOPP. The Transport Aircraft System OPTimization (TASOPT) [7] is being used to supply the performance parameters ANOPP requires. This tool jointly optimizes the airframe, engine, and full flight trajectory of a “tube and wing” transport aircraft using physics-based computations, and is therefore useful for predicting weight, aerodynamics and performance without the need for traditional empirical drag and weight prediction methods. A tool to translate the performance outputs from TASOPT into inputs for ANOPP has been created as part of this research. The analysis architecture for the integrated TASOPT and ANOPP tool is summarized in Figure 3. The full set of input parameters required by ANOPP is provided in Table 1, along with the source for each parameter in the current implementation of the tool.

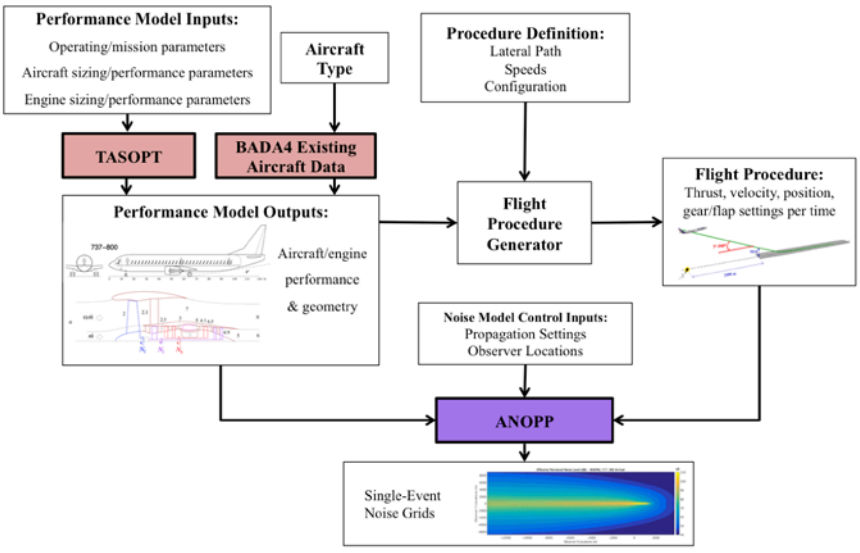

Figure 3. Integrated TASOPT and ANOPP analysis process to generate high fidelity approach and departure noise estimates

Table 1. ANOPP Parameters by Category and Source.

Parameter Category	Parameter	TASOPT Direct Output	Computed from TASOPT Output	User Input	ANOPP Default
Engine Performance	Fuel to Air Ratio of Core Inlet/Exit, Turbine Inlet/Exit, Jet Primary/Secondary Stream	*			
	Mass Flow Rate of Fan Inlet/Exit, Core Inlet/Exit, Turbine Inlet/Exit, Jet Primary/Secondary Stream	*			
	Total Pressure of Core Inlet/Exit, Turbine Exit, Jet Primary/Secondary Stream	*			
	Total Temperature of Fan Inlet/Exit, Core Inlet/Exit, Turbine Inlet/Exit, Jet Primary/Secondary Stream	*			
	Rotation Rate of Fan Inlet, Turbine Inlet/Exit	*			
	Fan Rotor Relative Tip Mach Number		*		
Engine Geometry	Area of Core Inlet/Exit, Turbine Exit, Jet Primary/Secondary stream	*			
	Number of Engines	*			
	Fan Rotor Diameter	*		*	
	Jet Plug Area	*		*	
	Number of Fan Rotor Blades			*	*
	Number of Fan Stator Vanes			*	*
	Fan Rotor-Stator Spacing			*	*
	Number of Turbine Stages			*	*
	Mean Axial Rotor Blade Chord of the Last Turbine Stage			*	*
Aircraft Geometry	Aircraft Total Weight	*		*	
	Area/Span of Wing, Horizontal, Vertical	*			
	Area/Span of Flaps		*		
	Number of Wheels of Main/Nose Gear		*		
	Number of Struts of Main/Nose Gear		*		
	Wheel Diameter of Main/Nose Gear		*		
	Strut Length of Main/Nose Gear		*		
	Leading Edge/Trailing Edge x, y, z Coordinates of Wing, Flap, Tab		*		
Aircraft Performance	Aircraft x, y, z Position Coordinates/Time	*		*	
	Aircraft Velocity/Time	*		*	
	Aircraft Glideslope/Time	*		*	
	Aircraft Thrust/Time	*		*	
	Aircraft Angle of Attack/Time		*		
	Aircraft Gear/Flap Configuration/Altitude			*	
Propagation Effects	Ground Level Pressure/Temperature	*		*	
	Relative Humidity			*	
	Flag to Consider Absorption, Ground Effects			*	
	Ground Surface Type			*	
	Specific Flow Resistance of the Ground			*	*
Misc.	Frequency			*	*
	Directivity Angles			*	*
	Observer x, y, z Grid			*	
	Noise Computation Methods			*	
	Type of Outputted Noise Contour			*	

Along with the outputs from TASOPT, the observer grid and propagation settings (atmosphere definition, shielding effects, etc.) and the flight procedure thrust, velocity, and position settings as a function of time must also be supplied. A generator was created to compute the specifics of a flight procedure using a basic force-balance model to determine required thrust levels given a user-specified flight-path angle and velocity. Presently, the Base of Aircraft Data (BADA) Family 4 [8] is supplying drag increases with changes in flap and gear configurations for existing aircraft. A modification to TASOPT, which currently does not model the effects of high-lift devices, is under development to supply drag increment estimates for high-lift configurations.

To verify the accuracy of this integrated system, results have been compared to FAA certification noise data at the standard "flyover", "approach" and "sideline" locations along with weight, configuration and thrust levels for many aircraft types. Sample results shown in **Error! Reference source not found.** comparing the TASOPT-ANOPP framework results with the FAA certification data for Boeing 737-800 and 777-300 indicate agreement to within 4.51 EPNdB for each of these certification points for these aircraft.

Table 2. Comparison between EPNL noise values generated by the TASOPT-ANOPP model, AEDT, and the FAA Noise Certification database

		FAA Cert. Data (dB)	TASOPT/ANOPP Model Results EPNL (dB)					ANOPP vs. Cert. (dB)	AEDT EPNL (dB)	AEDT vs. Cert. (dB)
			Fan	Airframe	Core	Jet	Total			
Boeing 737-800	**Flyover**	**86.7**	83.0	77.9	79.4	69.6	**87.1**	+0.1	**86.9**	+0.2
TO/AP Wt: 172300/146300 lbs	**Approach**	**96.8**	94.1	90.7	85.9	70.0	**97.2**	+0.4	**95.4**	-1.4
Engine: CFM56-7B26	**Lateral***	**93.1**	92.5	71.3	87.7	92.9	**97.9**	+4.8	**100.6**	+7.5
Boeing 777-300	**Flyover**	**94.2**	91.5	84.5	88.6	76.2	**95.1**	+0.9	pending	pending
TO/AP Wt: 636100/524000 lbs	**Approach**	**100.4**	98.5	95.2	92.8	67.1	**100.9**	+0.5	pending	pending
Engine: RR Trent 892	**Lateral***	**96.9**	98.1	77.5	93.4	91.4	**101.5**	+4.6	pending	pending
Embraer 195	**Flyover**	**86.5**	81.9	75.7	76.8	68.7	**86.4**	-0.1	pending	pending
TO/AP Wt: 111970/99200 lbs	**Approach**	**92.8**	90.6	81.2	80.7	64.6	**92.7**	-0.1	pending	pending
Engine: CF34-10E5	**Lateral***	**91.8**	90.6	69.3	81.3	81.7	**93.9**	+2.1	pending	pending

Flight profile generation and thrust calculation.

In order to obtain the flight profile data for ANOPP, a flight profile generator was created with the capability of computing the thrust profile from existing radar track data or for the generation of new profiles given a set of user specified segment requirements. The provided radar lateral track, altitude, and indicated airspeed of selected flights are processed through the procedure generator to compute the required thrust at each time stamp segment using a force balance model based on the velocity, altitude, acceleration, flight path angle, and configuration at that segment. If flap and gear configuration information is not available, the flap configuration changes are assumed governed by the weight and speed windows for the given aircraft type assuming the flap speed ranges shown in Table 3

Table 3. Flap Speed Ranges Used for Each Aircraft Type. Max Values Obtained from Flight Crew Operating and Training Manuals for Each Type, [9], [10]

Boeing 737-800 Flap Speed Ranges (kts)		Airbus A320 Flap Speed Ranges (kts)	
Flaps 1	210 – 250	CONF 1	210 – 230
Flaps 5	200 – 250	CONF 2	180 – 200
Flaps 10	190 – 210	CONF 3	165 – 185
Flaps 15	170 – 200	FULL	155 – 177
Flaps 25	160 – 190		
Flaps 30	150 – 175		

To compute profile information for a user-defined profile, the user specifies a set of requirements to define a flight segment. These include thrust, configuration, velocity and acceleration, position, and flight path angle. Given enough defined requirements, the profile generator computes the remaining parameters not yet specified using the same model as in the case when flight radar tracks are given, including takeoff and landing rolls. This is repeated for any number of profile segments—the end parameters of the first defined segment become the initial parameters of the next segment.

TASOPT/ANOPP Model Validation with FAA Noise Certification Data

The integrator tool is currently configured to predict fan, airframe, core, jet, and turbine noise using TASOPT version 2.13 and ANOPP Level 30 version 3. As part of the validation process for the TASOPT and ANOPP noise model, modeled EPNL values were compared with arrival and departure certification data from official FAA noise certification records [11]. The certification noise data are recorded at specific locations with prescribed weight, configuration, and thrust levels stipulated in 14 CFR 36 Appendix B (http://www.ecfr.gov/cgi-bin/text-idx?rgn=div5&node=14:1.0.1.3.19#ap14.1.36_11583.b). Certification data for three observer locations are provided for each aircraft type: an arrival observer directly under the approach path (approach reference), a departure observer offset from the runway at the loudest point of the departure (lateral reference), and an observer directly under the departure flight path (flyover reference). The location of these observers is defined in the federal regulations and shown in Figure 4.

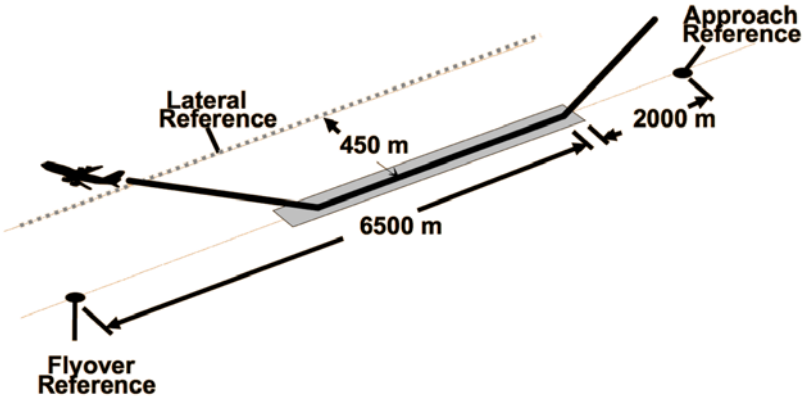

Figure 4. Standard EPNL measurement locations prescribed in FAR Part 36 for noise certification in the United States.

Three aircraft types were modeled in TASOPT: the Boeing 737-800 with CFM56-7B26 Engines, the Boeing 777-300 with Rolls Royce Trend 892 engines, and the Embraer 195 with General Electric CF34-10E5 engines. These three types represent a wide range of thrust, performance, and weight categories to cover a variety of approach and departure trajectory scenarios. Each of the aircraft was simulated on the certification standard noise arrival and departure trajectories as defined in FAR Part 36 within ANOPP. In addition, the same arrival and departure trajectories were implemented in AEDT for the 737-800 as an additional point of comparison. In both cases, the arrival and departure trajectories were fully defined in terms of speed, altitude, thrust, and aircraft configuration as a function of time and distance in the procedure. The modeled noise results are compared to published noise certification value in Table 2.

The difference between ANOPP-modeled noise and the noise certification database was within 1 dB for all three aircraft types in the flyover and approach cases. The sideline case showed larger differences (as high as 4.8 dB), with ANOPP appearing to overpredict noise in these high-thrust cases. As a point of comparison, the 737-800 certification cases were also run in AEDT. The magnitude of differences between the certification and modeled values was similar for this industry-standard noise model. Consultation with industry experts (aircraft manufacturer noise technicians and noise model developers at the DOT Volpe Research Center) indicated that this noise measurement location is particularly sensitive to exact aircraft trajectory, making duplication of flight test conditions in noise models particularly difficult. In addition, aircraft flying noise certification test profiles do not always fly the procedures exactly as defined in FAR Part 36, substituting alternative procedures and test plans to generate the ultimate certification value. As a results of discussions with industry experts and similar results from

AEDT, the consistency between TASOPT/ANOPP and FAA certification values was deemed adequate to continue noise analysis of advanced operational procedures with the tool.

Noise Measurement Comparison at Boston Logan Airport

Much of the potential noise impact from advanced operational procedures occurs in areas farther from the airport than the reference points captured by certification noise values. As a result, it was desirable to obtain a reference dataset of operational noise measurements for aircraft following actual terminal-area procedures for comparison with modeled results. In conjunction with research at MIT Lincoln Laboratories in support of development of the Delayed Deceleration Approach concept, three Brüel & Kjær Noise Sentinel monitor systems were placed at the NM locations illustrated in Figure 5. Noise monitor locations on the approach path to Rwy 22R and 22L at Boston Logan Airport.. These locations were selected based on a study of aircraft overflight density, with target areas chosen for monitor deployment at ranges from 10-30 nmi track distance from the airport. Within these areas, potential test sites were identified including both private residences and businesses. The characteristics sought in a test site included high densities of aircraft over-flights, low background noise level, easy accessibility, ready power supply and security (the latter two characteristics given the need to deploy systems for extended periods of time). As site locations were investigated, it was determined that much of the target area to runways 4L/4R was unpopulated land which lacked easy access or power supply. Therefore it was decided to focus the campaign on flights landing on runways 22L/22R. The final locations chosen were three private residences which could provide power and a secure location for the monitors. Noise Monitor A (NM-A) is approximately 13 nmi flight track distance from runway 22, while NM-B and NM-C are approximately 16 and 20 nmi from touchdown for a typical downwind segment, but could be a much larger flight track distance from touchdown if an extended downwind segment was being used.

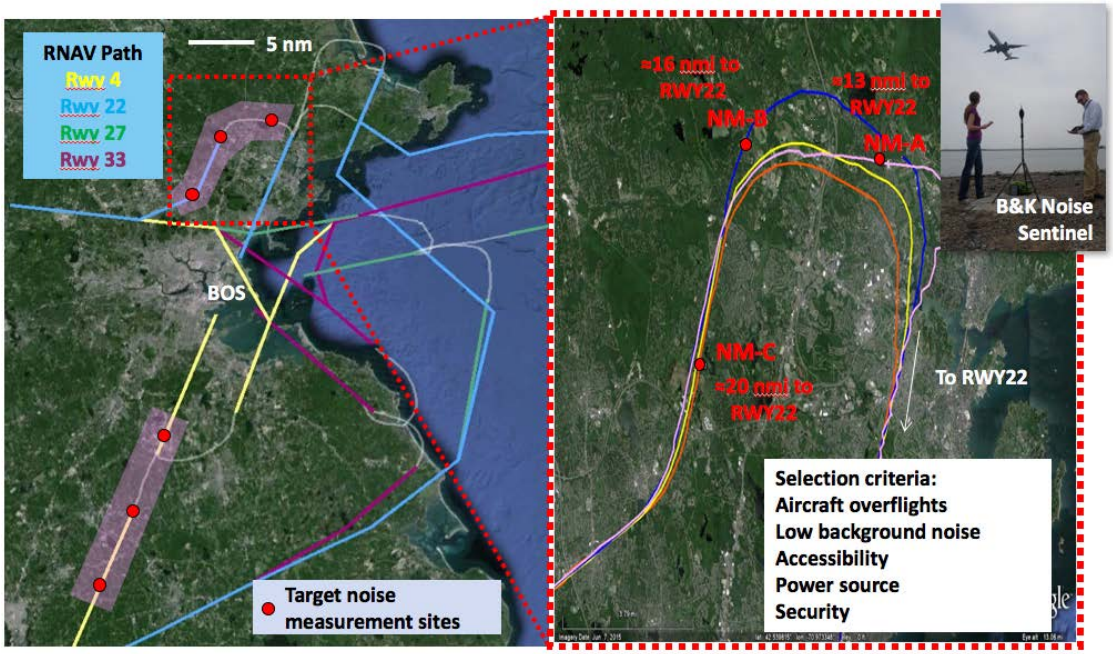

Figure 5. Noise monitor locations on the approach path to Rwy 22R and 22L at Boston Logan Airport.

The noise monitors collected 1-second equivalent sound level (Leq) noise data 24-hours a day which was streamed to a web server in real-time via a cellular modem. Flight track radar data was used to correlate a noise event to a specific aircraft and to determine its altitude and speed as it overflew the monitor. Raw PDARS data with 4.8 second update rate was used for this flight association. The groundspeed of the aircraft was calculated based on position information as a function of time. This groundspeed was converted to true airspeed using a wind vector determined from the North American Regional Reanalysis (NARR) data interpolated in space and time to the aircraft position, and from there was converted to indicated airspeed (IAS) using the appropriate atmospheric corrections. All the results shown below are displaying IAS.

For any flight overflying one of the monitors to within 0.5 nmi lateral distance, the timestamp was taken from PDARS at the time it was closest to the monitor and this timestamp was matched to the noise data. Then a window was searched for the maximum noise value within +/- 10 seconds of that timestamp. The point with the highest 1-second Leq reading was chosen as the appropriate timestamp and the 1-second Leq noise value at this time was set to be Lmax. The maximum noise levels generally occurred after the original timestamp by several seconds. Figure 6 shows sample flight tracks for four aircraft that flew over all three monitors. Two of those tracks are mapped to the noise data to show the noise events from those aircraft at each monitor.

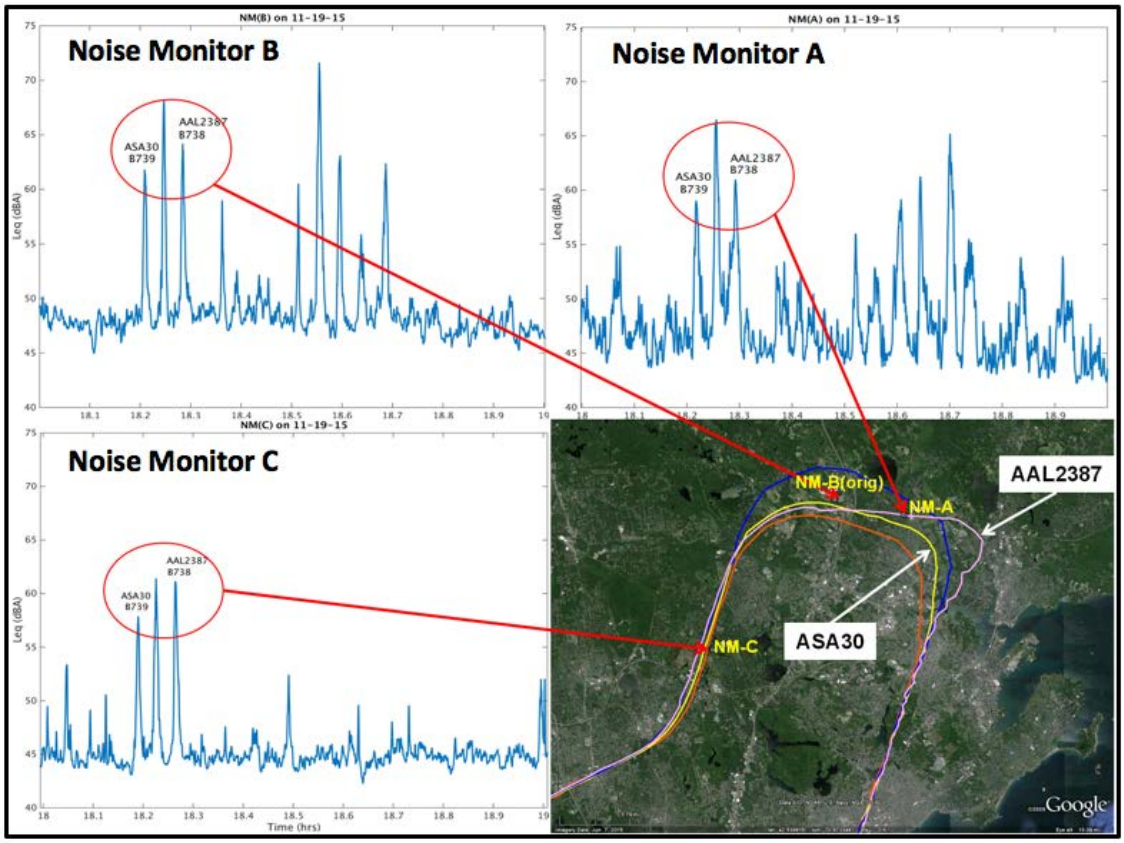

Figure 6. Example equivalent sound level records from each of the three noise monitoring stations deployed on the approach path to Boston Logan Airport.

Noise measurement results were collected for all aircraft types and airlines serving Boston Logan Airport that overflew the noise monitors on approach to Runways 22L and 22R during the sample collection period. The results were then segregated by aircraft type. Scatter in the results of 10 dB or more was observed for all common aircraft types for both sound exposure level (SEL) and maximum noise level (Lmax) metrics. **Error! Reference source not found.** shows example SEL measurements at Noise Monitor B, including overflights occurring throughout the three-month measurement period displayed as a function of airspeed.

In order to evaluate the ANOPP model against the noise monitor results, four specific flights were selected for modeling. For two aircraft types, the A320 and B737, example flights from the BOS noise measurement campaign were chosen based on their average speeds and the number of noise monitors the aircraft flew over. First the flights with the lowest and highest 5% of average airspeed were selected. From those subsets, one flight was chosen that followed a large fraction of the QUABN3 RNAV approach procedure and flew over at least two noise monitors. The lower average airspeed flights often were ones flying extended downwind legs.

The lateral track, altitude and indicated airspeed of the selected flights were processed through the model in order to develop noise contours for Lmax. The flap configuration changes were assumed governed by the weight and speed windows for each aircraft type (assuming the flap speed ranges shown in **Error! Reference source not found.**) and the landing gear was assumed to be deployed at 2000 ft. The results for an example A320 with an approximately 10 nmi downwind leg are shown in Figure 8.

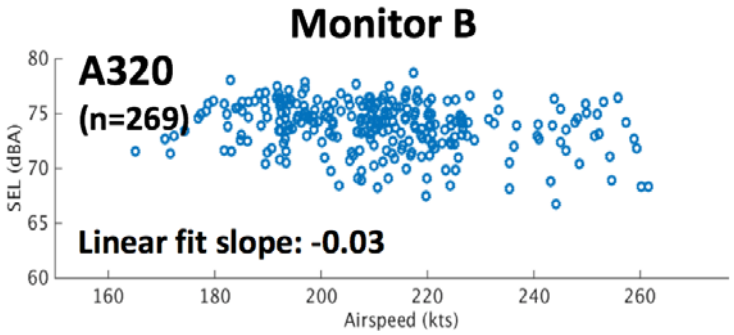

Figure 7. Measured sound exposure levels (SEL) for A320 flights over Noise Monitor B during noise measurement campaign.

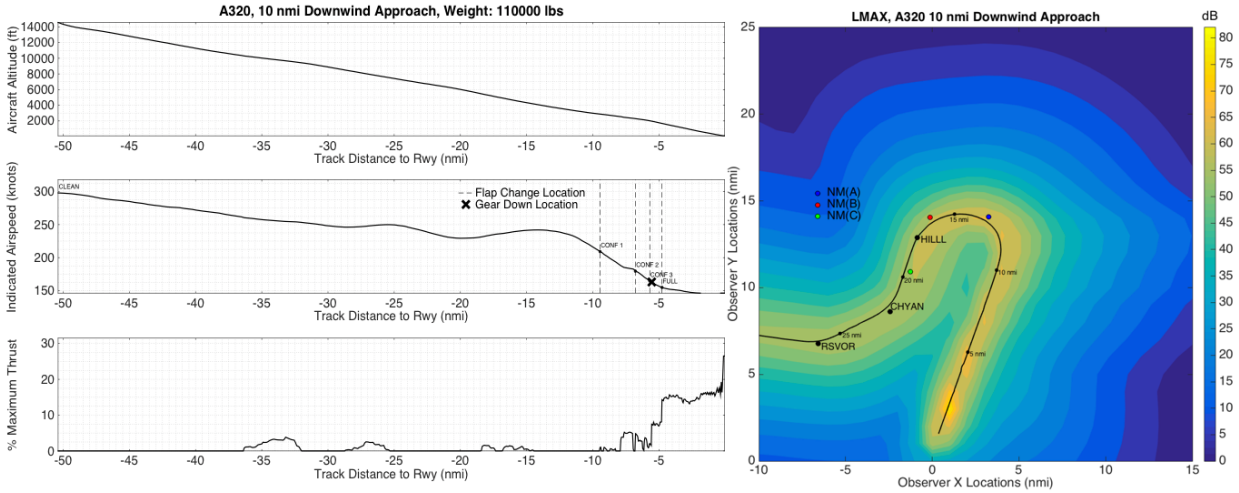

Figure 8. A320 Standard Downwind Approach Flight Profile (left) and Lmax Contour (right)

The computed values of Lmax from the noise contours as the aircraft passes over each noise monitor are shown in Table 4 Those values are compared with the measured values recorded by the noise monitors. Comparison between the measured and modeled Lmax data at these locations are within 6 dBA agreement across all cases, i.e., within the scatter seen in the measured data. Consultation with noise modeling experts in academia, at aircraft manufacturers, and at NASA provided insight about the cause the large scatter in noise measurement results. Two primary factors influence the variation:
Thrust differences between aircraft flying the same published approach based on pilot technique and aircraft energy state.
Differences in sound propagation due to atmospheric conditions, shielding in the vicinity of the observer on the surface, wind, etc.

While the TASOPT/ANOPP model was capable of estimating thrust levels for each specific trajectory (the first significant cause of scatter), daily variation in propagation characteristics could not be fully captured.

Table 4. Comparison between noise monitor measurements for four A320 arrivals at Boston Logan Airport and the same procedures modelled using TASOPT and ANOPP.

L_{max}(dBA)	NM (A)		NM (B)		NM (C)		Difference (Measured minus ANOPP Modeled)		
	Measured	ANOPP	Measured	ANOPP	Measured	ANOPP	NM(A)	NM(B)	NM(C)
20 nmi Downwind A320	-	-	62.4	57.3	61.0	56.6	-	5.1	4.4
10 nmi Downwind A320	61.9	64.0	-	-	54.3	57.7	-2.1	-	-3.4
20 nmi Downwind B737	-	-	59.1	57.8	60.7	55.6	-	1.3	5.1
10 nmi Downwind B737	69.0	62.4	66.50	62.3	60.1	58.9	6.7	4.2	1.2

Comparison of Engine and Fan Noise Models within ANOPP

ANOPP is a modular noise analysis tool that independently calculates and combines noise from a variety of sources and physical processes. Each module can be individually refined, modified, or replaced based on research in underlying acoustics and computation. This has resulted in several modules for particular noise sources with multiple methods available, normally based on different calculation methods and tuned for specific use cases. For modules where different noise modules are available without a clear indication of which is preferable for the analysis of advanced operational procedures, additional analysis of the candidate modules was necessary.

A series of calculations were performed to examine the differences in noise predictions from both engine and airframe noise sources. In particular, the predictions based on the newer source models in ANOPP were compared with the level predictions from the original FAA Component Method. The engine noise sources considered were fan inlet and exhaust noise and jet noise. Airframe noise sources included flap and slat noise, landing gear noise, and trailing edge noise sources.

Fan Noise

The original fan noise model in ANOPP was developed by Heidmann [12]. The contributions to the total fan noise include inlet broadband noise (INBB), inlet discrete tone noise (INRS), inlet combination tone noise (INCT), discharge broadband noise (DBB), and discharge discrete tone noise (DRS). Inlet and discharge broadband noise are associated with the random unsteady flow passing the blades, turbulence on the wall and in the blade boundary layers, in the blade wakes and vortices, and also from the distorted inlet flow. Inlet and discharge discrete tones are associated with lift fluctuations on the rotor or stator blades. Inlet combination tones are associated with the shock waves that form at the tips of rotors with supersonic tip speeds. The spectrum of INCT noise contains harmonics of the shaft rotational speed rather than the blade passing frequency.

In ANOPP there are four fan noise prediction options. These are the original Heidmann method [12], a modification by Allied Signal for smaller engines (small fan method) [13], a further modification by General Electric for large modern turbofans (large fan method) [14], and the most recent update based on the Source Diagnostic Test fan model data [15]. Predictions were made for the sideline noise certification location for takeoff of a Boeing 737-800. The aircraft flight paths for sideline and cutback trajectories are shown in Figure 9.

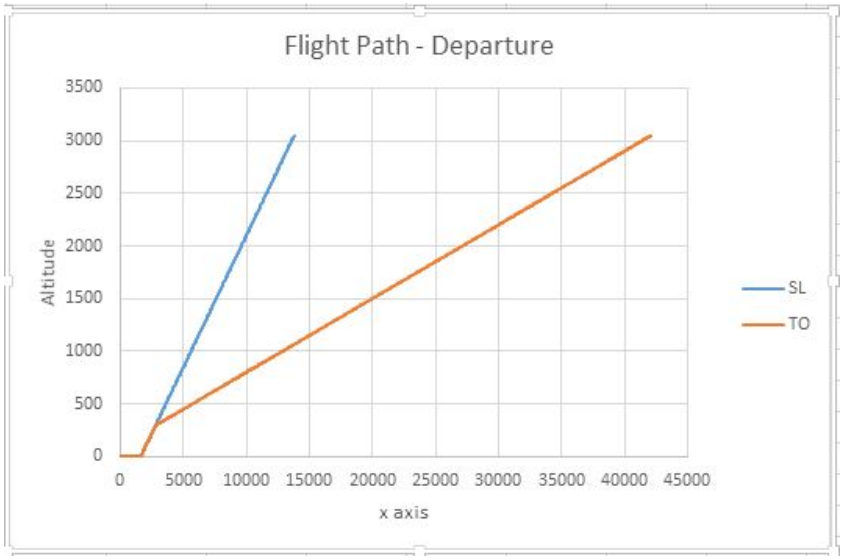

Figure 9. Departure flight paths for Boeing 737-800.

It was found that the INCT noise was over-predicted by the Krejsa model. However, if acoustic treatment was also included, using the TREAT module in ANOPP, then the predictions agreed well with the FAA certification value and reasonably well with the large fan model (without acoustic treatment). This shown in Table 5.

Table 5. EPNL Fan noise only at sideline location (2845, 450, 0)

Noise Source	Large Fan	Krejsa
Broadband	86.90	86.84
Broadband+tones	94.87	100.15
Broadband+tones+TREAT	92.54	88.95
FAA certification value	88.77	

Airframe Noise

Two approaches are available in ANOPP for the prediction of airframe noise. These are the original Fink or FAA Component model [16], and the Boeing Airframe Noise Model, which is based on several studies that are referenced below.
The Fink model expresses the mean square pressure from all the components of airframe noise in the form:

$$\langle p^2(rs,f,\theta,\phi)\rangle = \frac{\Pi^*}{4\pi r_s^{*2}} \frac{D(\theta,\phi)F(S)}{(1-M_\infty cos(\theta))^4},$$

$$S = \frac{fL}{M_\infty c_\infty}(1-M_\infty cos(\theta)), \qquad \text{(Eq. 1)}$$

$$\Pi^* = K(M_\infty)^a G.$$

Here, Π^* is the acoustic power, $D(\theta,\phi)$ is the directivity factor, $F(S)$ is the spectrum shape as a function of the Doppler shifted Strouhal number S, r_s^* is the source to observer distance, K and a are empirical constants and G contains geometry information for each airframe noise source.

The general forms for the Boeing Airframe Noise model all take similar forms. The models are described in some detail in several reports [17], [18], [19]. For example, the flap side edge noise power spectral density is given by:

$$G_{pp} = A_G A_F W(M_\infty) F(f_D, M_\infty) D(\theta,\phi) \frac{l^2 C_{flap}}{r_s^2 (1 - M_\infty cos\theta)^2}. \qquad \text{(Eq. 2)}$$

A_G and A_F are amplitude functions that depend on the geometry and flow conditions respectively. $W(M)_\infty$ gives the dependence on flight Mach number, $F(f_D, M_\infty)$ provides the spectrum shape, $D(\theta,\phi)$ is the directivity function, C_{flap} is the flap chord and l is a characteristic length scale for the low and high frequency contributions to the spectrum. For example, $l = C_{flap}$ for the low frequencies and $l = h$ for the high frequencies, where h is the flap thickness.

A parametric study was conducted to examine the effect of the different geometric and flow parameters on the predicted airframe noise. For example, Table 6 shows the effect of flap chord length on the SPL and EPNL at the approach certification location. Here, the flap deflection is 40 degrees, $h = 0.141$ m and the flap span equals 6 m. It would be expected that, based on the general noise prediction formula, the levels should scale with the cube of the flap chord. However, this is not the case. Unfortunately, the implementation in ANOPP contains many empirical constants that are proprietary to Boeing, so the reason for this apparent discrepancy is very difficult to determine.

Table 6. Variation of flap side edge noise level with flap chord length.

Chord Length	0.235m	0.47m	0.94m	1.88m	3.76m
SPL	86.03	92.31	97.82	101.69	103.77
EPNL	89.03	94.0	98.35	101.46	102.96

For a given set of flap dimensions the Fink and Boeing models give EPNL predictions that differ by less than 2 dB.

The Fink model for landing gear noise is based on the dimensions of the wheel and main strut alone. Whereas the Boeing model allows the user to input a larger set of landing gear noise components. In addition, the Boeing model calculates contributions to the overall spectrum from large, medium and small landing gear components. The general formulation for the mean squared pressure is given by:

$$\langle p^2 \rangle = \sum_{i=1}^{3} \frac{M_i^6 P_i}{r_s^2 (1.0 - M_i cos\theta)^4}, \qquad P_i = \beta S_i D(\theta,\phi) F(St). \qquad \text{(Eq. 3)}$$

This gives the contributions from the three components. The surface area of the components is given by S_i, $i = 1,2,3$. S_L for the low frequencies is based on the tire diameter, S_M is the averaged surface area of all the components, and S_H is based on a complexity factor and is some percentage of the average diameter. This method is the "detailed" method. If all the landing gear components are not listed, then the dimension of the largest gear component, such as the main strut, is used to predict the surface areas for the medium and high frequency components. This is the "estimated" method. Table 7 shows a comparison of EPNL predictions at the approach certification point using the Fink and Boeing methods.

Table 7. EPNL at approach certification location (-2000, 0, 0)

Fink	Boeing (detailed)	Boeing (estimated)	FAA certification value
84.1	79.52	79.5	82.7

Comparison of Noise Results in AEDT and ANOPP

One of the key objectives of this research has been to develop methods for quantifying noise impacts from advanced operating procedures that are not readily modeled with existing NPD-based methods. To evaluate the difference between the modular physics-based ANOPP model and the NPD-based AEDT method, an example arrival and departure profile were evaluated using both tools. In both cases, identical profile definitions were analyzed using both tools. Airspeed, altitude, thrust, and configuration were held constant between the two tools for the purpose of comparison. The noise observation grid and resolution was also consistent between runs, allowing direct comparison of model outputs.

Arrival Procedure Comparison in AEDT and ANOPP

For the arrival comparison case, a typical continuous descent approach profile was implemented in both ANOPP and AEDT. The aircraft follows a straight-in three-degree glideslope from 6000 feet until touchdown, decelerating from 240 knots to VREF+10 knots so as to be stabilized at the target final approach speed before a notional ILS outer marker at 2000 feet above ground level. The associated thrust and flap configuration are computed using the kinematic profile generation method described above. The resulting trajectory is shown in blue in Figure 10.

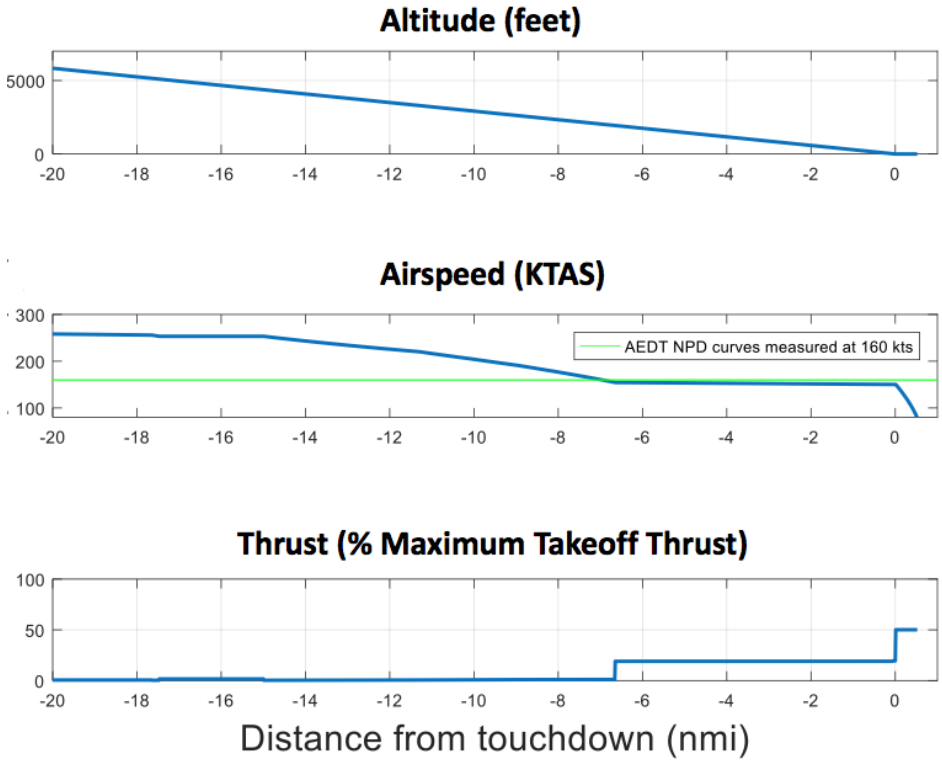

Figure 10. Trajectory definition for arrival procedure used in ANOPP and AEDT comparison.

In the NPD method for modeling noise, both airframe and engine noise components are combined into a single lookup table as a function of thrust level and observer distance. Airframe noise varies as a function of speed, meaning that the NPD dataset for approach conditions must be referenced to a specific airspeed and aerodynamic configuration. In accordance with SAE Standard 1845a, the reference speed used for approach procedures is 160 knots true airspeed with the aircraft in landing configuration. This reference speed is shown as a green horizontal line in Figure 10. Due to the variability of noise with speed and configuration, it is expected that NPD-based methods capture total noise most accurately near this reference speed with decreasing accuracy as the aircraft speed up or changes configuration.

Figure 11 shows the SEL noise contours for the example arrival procedure as calculated by both ANOPP and AEDT. The difference between these two contours is shown in Figure 12. The ANOPP noise prediction is louder than the AEDT prediction at all observer locations. However, the magnitude of the difference varies substantially depending on the distance to touchdown. From roughly 7nm on final until touchdown, the ANOPP and AEDT predictions are within 5 dB SEL. Outside of 10nm, however, the difference between the two is 10dB SEL or larger.

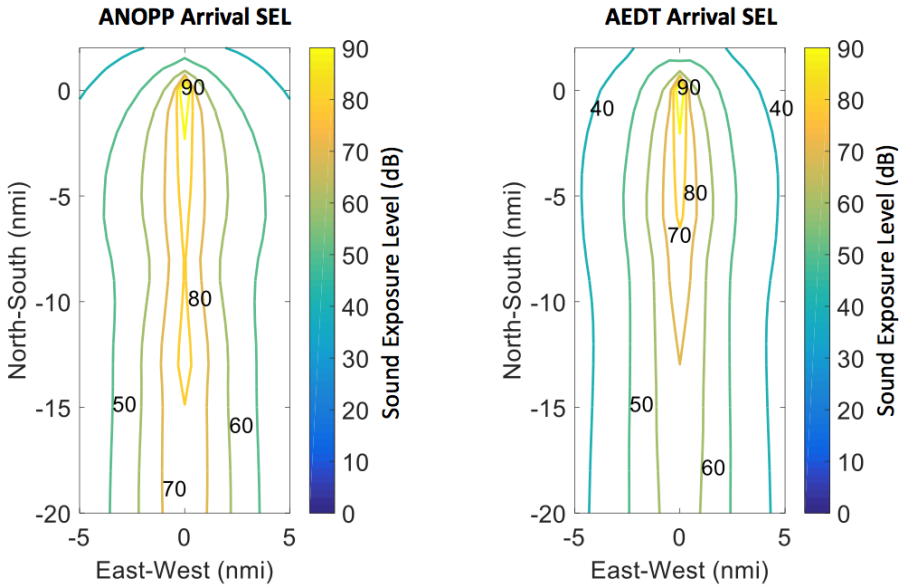

Figure 11. Sound Exposure Level contours generated by ANOPP and AEDT for an identical sample arrival procedure

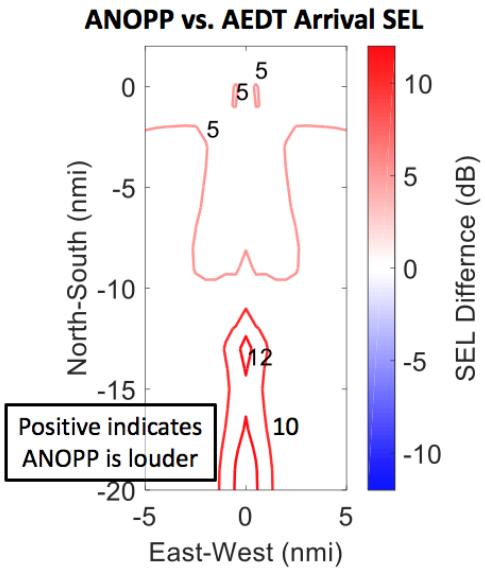

Figure 12. Difference plot between ANOPP and AEDT SEL results for an identical sample arrival procedure

The difference between the two models at distances farther from touchdown is likely attributable to the standardized speed of 160 knots represented by NPD datasets. At earlier phases of the approach when the speed is higher, physics-based

methods such as ANOPP are designed to capture changing aerodynamic noise effects while NPD-based methods such as AEDT apply the same lookup tables used for slower speeds. Thus, the higher airframe noise predicted by ANOPP is ignored by AEDT, resulting in larger discrepancies in phases of the approach where airspeed is substantially higher than 160 knots. This is a key difference between AEDT and ANOPP, emphasizing the value of higher-fidelity noise modeling.

Departure Procedure Comparison in AEDT and ANOPP

For the departure comparison case, a representative trajectory was selected for a Boeing 737-800 taking off from Washington National Airport (KDCA). The altitude and speed trace for the departure was taken from ASDE-X radar records at a 6-second resolution while the thrust was calculated using the kinematic profile generation method introduced in Section 0. The resulting trajectory is shown in Figure 13, with the corresponding ground track shown in Figure 14.

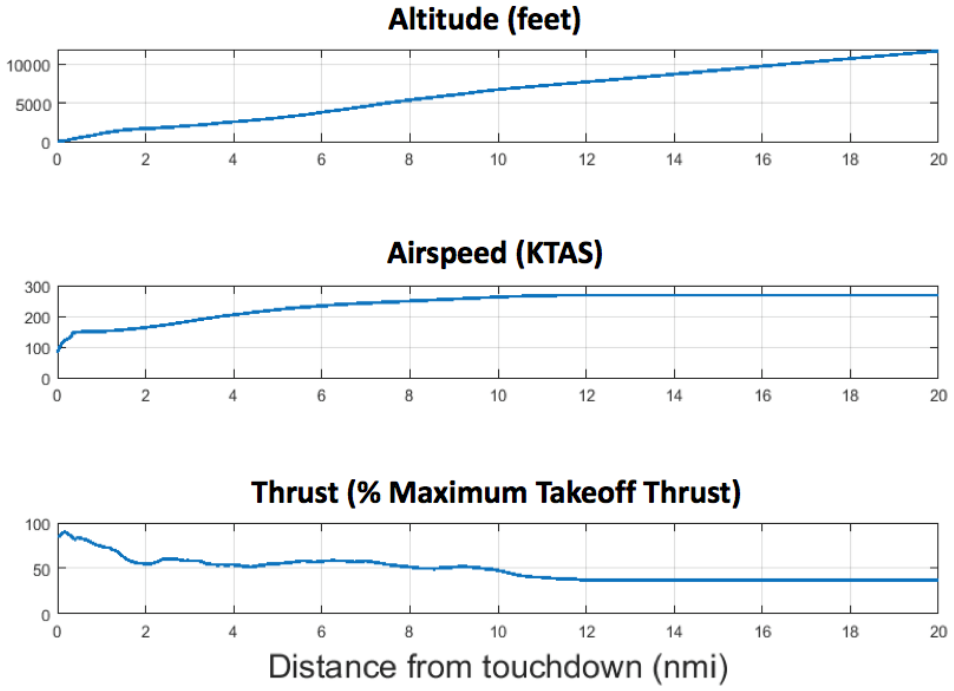

Figure 13. Trajectory definition for departure procedure used in ANOPP and AEDT comparison

Figure 15 shows the SEL noise contours for the example arrival procedure as calculated by both ANOPP and AEDT. The difference between these two contours is shown in Figure 16. The difference between the results from the two models is significantly smaller than in the approach case, with an absolute difference of less than 5dB SEL for all observers except for those in the immediate footprint of the airport (likely due to transient thrust modeling effects during the takeoff roll).

The key difference between arrival and departure noise signatures is the relative impact of engine noise compared to aerodynamic noise. In the arrival case, aerodynamic noise is a significant contributor to overall noise footprint. During departure, engine noise dominates airframe noise. NPD methods are designed to account for varying thrust levels as one of the interpolated lookup parameters, suggesting higher accuracy for cases with dominant engine noise. This example departure noise comparison between ANOPP and AEDT shows greater consistency than the arrival comparison presented in the previous section.

Figure 14. Ground track for departure procedure at DCA used in ANOPP and AEDT comparison.

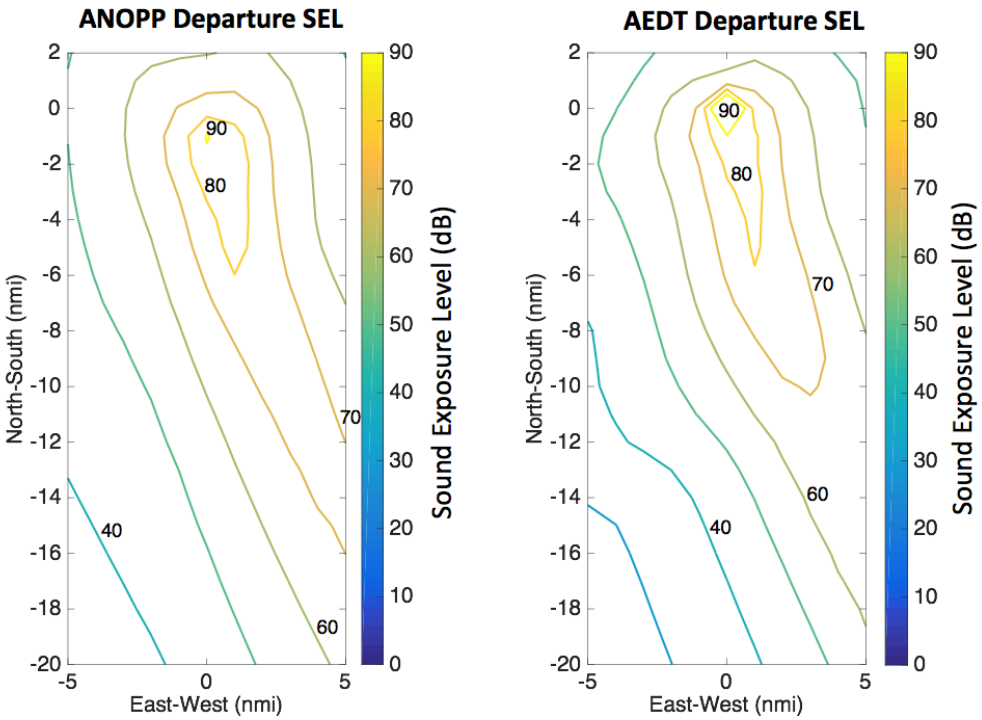

Figure 15. Sound Exposure Level contours generated by ANOPP and AEDT for an identical sample departure procedure.

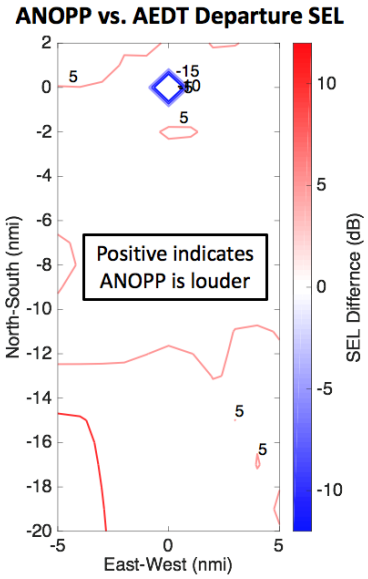

Figure 16. Difference plot between ANOPP and AEDT SEL results for an identical sample departure procedure.

Sample Procedure Results

Continuous Descent Approaches

In a continuous decent approach (CDA), the aircraft maintains a continuous descent from the cruise phase through landing. Conventional descent profiles normally have periods of level flight dictated by published arrival procedure, air traffic controller instructions, or pilot technique. The combination of increased altitude over greater portions of the approach and reduced thrust needed to fly on a level profile result in lower total fuel burn for the approach phase of flight. The modified profile also results in an impact on noise that can be modelled using the TASOPT-ANOPP model developed in this project.
In this example, a Boeing 737-800 flying a straight in approach at maximum landing weight (to maximize noise impacts) is modeled. In the first profile in Figure 17(a), the aircraft maintains an altitude of 2000 feet until localizer intercept at the final approach fix at 153 knots, after which the gear comes down and the aircraft descends to the runway. In the second profile

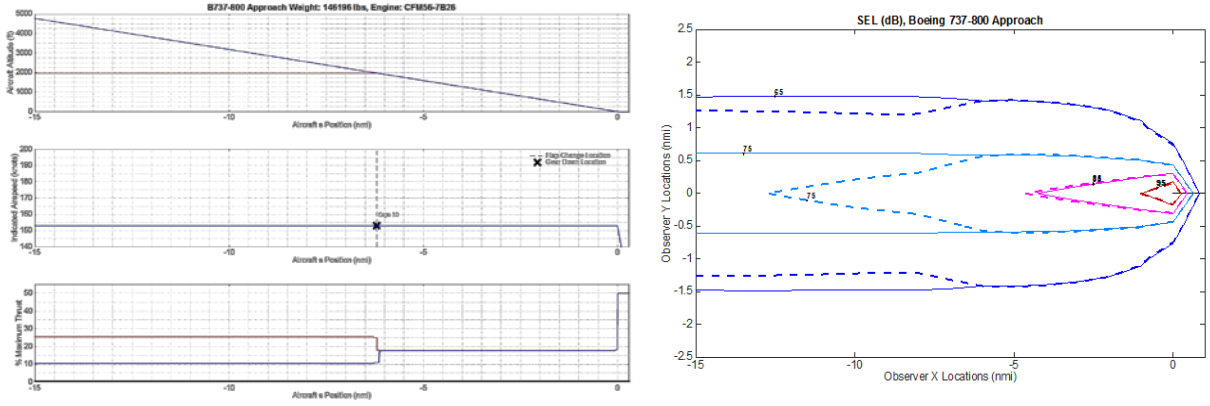

(a) (b)

Figure 17. Altitude, Velocity, and Thrust Profiles (a) and SEL Contours (b) of a Continuous Descent vs. Conventional Approach Profile

however, the aircraft is in a descent all the way to the runway, maintaining the same speed and dropping the gear at the same location as the level profile. The resulting thrust profiles show the computed thrust being higher for the conventional profile as expected. Noise contours were calculated for each profile, with SEL chosen as the metric to capture event duration effects. It is apparent that the decreased thrust and the greater altitude before the final approach fix of the continuous descent approach results in a decreased SEL (the two overlaid contours shown in Figure 17(b)) for the observers under this portion of the flight profile compared to the conventional approach.

Delayed-Deceleration Approaches

Some procedural changes have impacts on both aerodynamic and engine noise. The relative magnitude of changes from each source is not always obvious and the net effect is not normally captured by existing noise analysis tools. One key application for the noise modeling capability being developed in this project is the ability to analyze procedures in this category. An example of such an analysis is presented here.

In conventional descent and approach operations, aircraft often decelerate relatively early in their approach trajectory, as illustrated by the red region in Figure 18. This can be for a number of reasons, for example air traffic control may command early deceleration to give more time to space and sequence traffic flows onto the final approach or because of slower traffic ahead in the arrival stream. Earlier deceleration is accompanied by deployment of high-lift devices such as flaps, requiring higher engine thrust to counteract the resulting higher drag and giving rise to higher approach fuel burn and emissions. This can be avoided by implementing a Delayed Deceleration Approach (DDA) where the aircraft speed is kept higher for a longer time during the initial parts of the approach. The aircraft remain in a cleaner aerodynamic configuration for longer with associated lower fuel burn and emissions due to lower engine thrust requirements. The aircraft deceleration to the standard stabilized final approach speed occurs later in the approach, but still with sufficient time to comply with current stabilization criteria such that safety is not adversely affected. Prior analysis has shown that employing DDA procedures can reduce fuel burn in the arrival terminal area by as much as 50% relative to a typical earliest deceleration profile, and that this fuel burn reduction most strongly correlates with the airspeed profile and time flown with flaps extended [20].

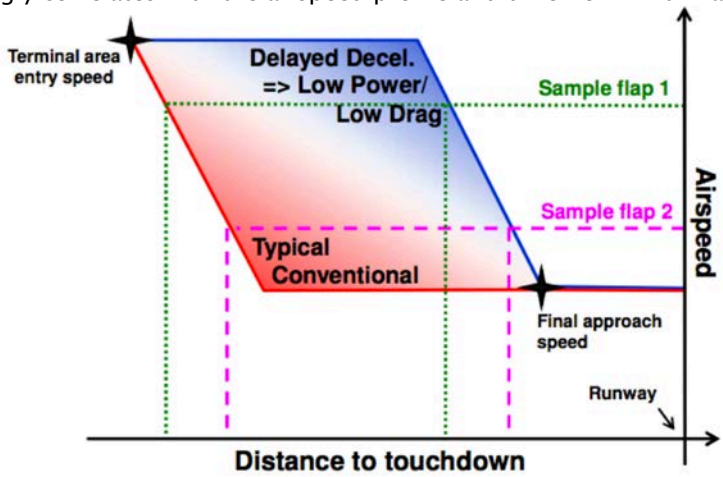

Figure 18. Delayed Deceleration Approach and Conventional Airspeed Profiles.

The noise impact of delayed deceleration approaches is not immediately obvious. A reduction in noise is expected from lower drag and thrust throughout most of the approach. Additionally, the delayed deployment of flaps and slats due to sustained high speeds is expected to reduce airframe noise hotspots. However, higher speeds increases overall aerodynamic noise in some phases of approach. The TASOPT/ANOPP tool is applied in this case to assess the net noise impact of the delayed deceleration approach, clarifying this tradeoff between engine and airframe noise.

The following two examples show the effects of employing delayed deceleration approaches on two example theoretical flight profiles. A Boeing 737-800 at maximum landing weight is again modeled. Figure 19 shows the effects of employing an early deceleration and delayed deceleration on the conventional approach profile from Figure 17. As seen in Figure 19(a),

both flights again maintain the same altitude of 2000 feet until localizer intercept at the final approach fix, after which the gear comes down and both aircraft descend to the runway. However, in the early deceleration case, the aircraft decelerates at the idle thrust setting provided by BADA 4 from 240 kts at the beginning of the profile until it reaches the final approach speed. It maintains that speed until the final approach fix. For the delayed deceleration case, the aircraft maintains a speed of 240 kts as long as possible and then decelerates at idle thrust to the final approach speed. From the final approach fix on, the speed profiles are identical. The thrust profiles show that, except for when the early deceleration case is at idle thrust during the initial deceleration, the thrust is lower for the delayed deceleration case as expected.

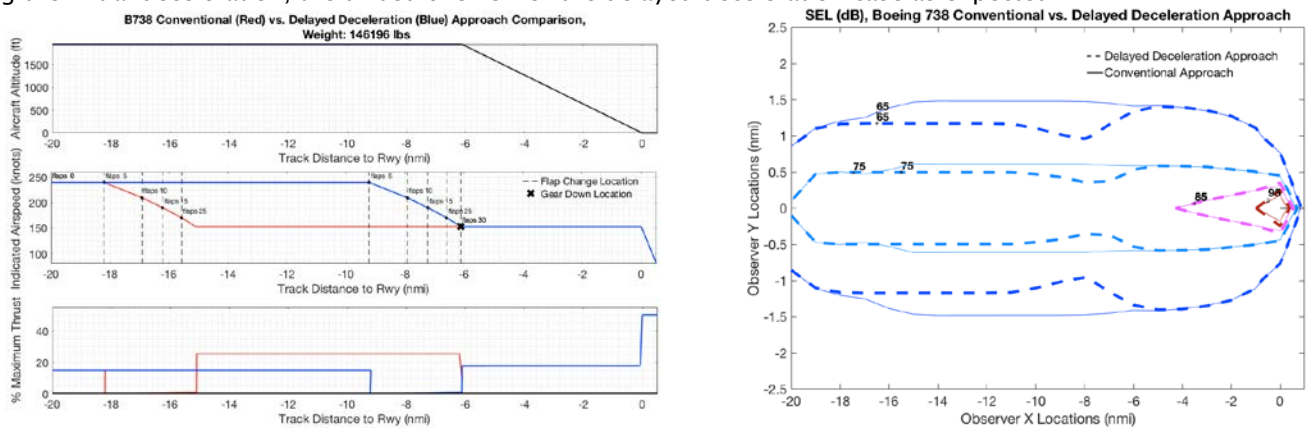

(a) (b)

Figure 19. Altitude, Velocity, and Thrust Profiles (a) and SEL Contours (b) of an Early and Delayed Deceleration Conventional Approach Profile.

The SEL contours of the early and delayed deceleration cases of the conventional approach profile are overlaid in Figure 19(b). In this example, the early deceleration case is as loud or louder in all regions than the delayed deceleration case. It is apparent that the reduction in thrust and resulting engine noise over much of the delayed deceleration profile is greater than the increase in airframe noise that results from the increased speed. Thus in this example, the delayed deceleration case provides a marginal noise benefit compared to the early deceleration case.

The final example in Figure 20 shows the effects of employing an early deceleration and delayed deceleration on a continuous descent profile. In the early deceleration case in Figure 20(a), the aircraft again decelerates at the idle thrust setting from 240 kts at the beginning of the profile until it reaches the final approach speed, while in the delayed deceleration case, the aircraft maintains a speed of 240 kts as long as possible and then decelerates at idle thrust to the final approach speed. From the final approach fix on, the speed profiles are again identical. The thrust profile again shows that except for when the early deceleration case is at idle thrust during the initial deceleration, the thrust is lower for the delayed deceleration case as expected. However, the difference in thrust between the early and delayed deceleration cases is less than in the conventional approach example.

The SEL contours of the early and delayed deceleration cases of the continuous descent approach profile are overlaid in in Figure 20(b). Unlike the conventional approach example, the delayed deceleration case in this example is as loud or slightly louder in all regions than the early deceleration case. In this case the increase in airframe noise that results from the increased speed reduction in the delayed deceleration profile is greater than the reduction in thrust and resulting engine noise. Thus in this example, the delayed deceleration case provides a small noise detriment compared to the early deceleration case.

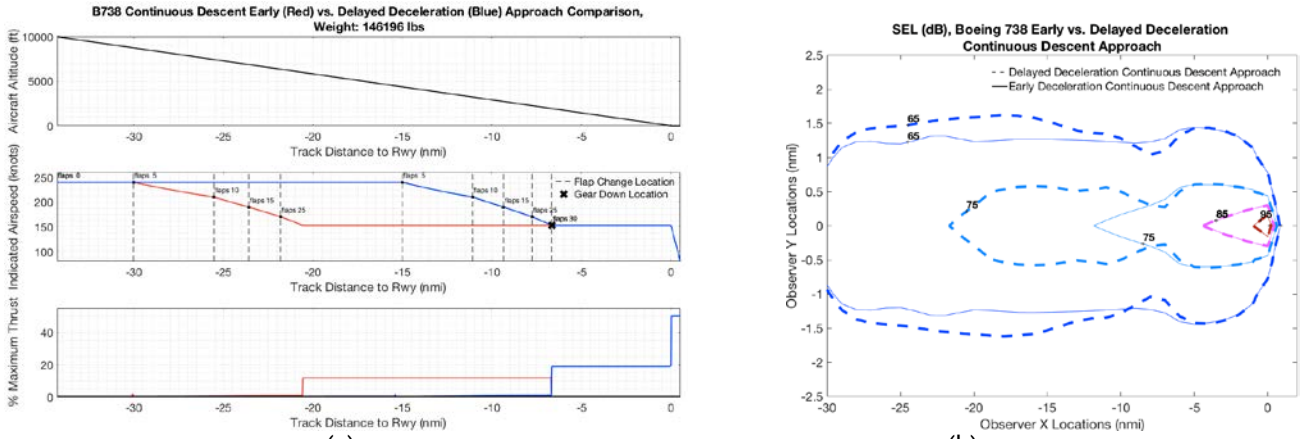

Figure 20. Altitude, Velocity, and Thrust Profiles (a) and SEL Contours (b) of an Early and Delayed Deceleration Continuous Descent Profile.

Modeling of Actual Approaches with Modified Speed Profiles

The integrated TASOPT-ANOPP noise model was also used to examine the effects of employing a delayed deceleration approach on a flight track into Boston Logan Airport following the QUABN3 RNAV into runway 22L and comparing it directly with an early deceleration case. The baseline (as-flown) A320 approach profile shown in **Error! Reference source not found.** is used as an example approach track definition (latitude, longitude, and altitude) to demonstrate the effect of speed and configuration on approach noise.

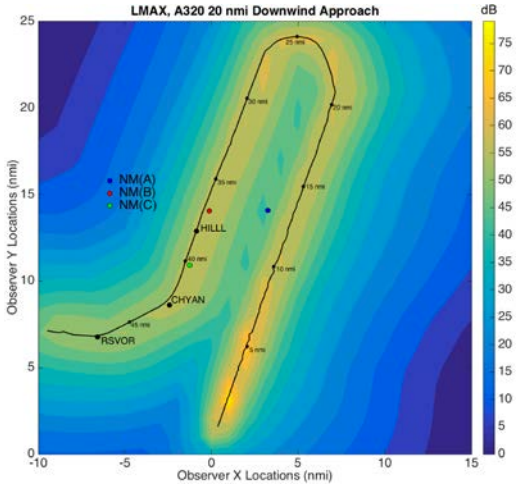

Figure 21. A320 approach procedure to Runway 22L at Boston Logan Airport with calculated maximum noise level contours overlaid for the as-flown speed profile.

The same altitude and lateral profile as well as wind conditions of this flight track were used to create an early deceleration case where the aircraft starts decelerating at the start of the profile at idle thrust until it reaches the speed at the final approach fix of 150kts. Flaps are assumed to change at the maximum flap speeds shown in Table 3 in order to compute the shortest length needed to decelerate. Similarly, a delayed deceleration case where the aircraft maintains its initial speed of 220kts as long as possible and then decelerates at the idle thrust setting to the final approach speed is also modeled. From the final approach fix on, the speed and thrust profiles of both cases are identical. The altitude, speed, and thrust profiles

are overlaid and shown in Figure 22, where red represents the early deceleration case and blue represents the delayed deceleration case.

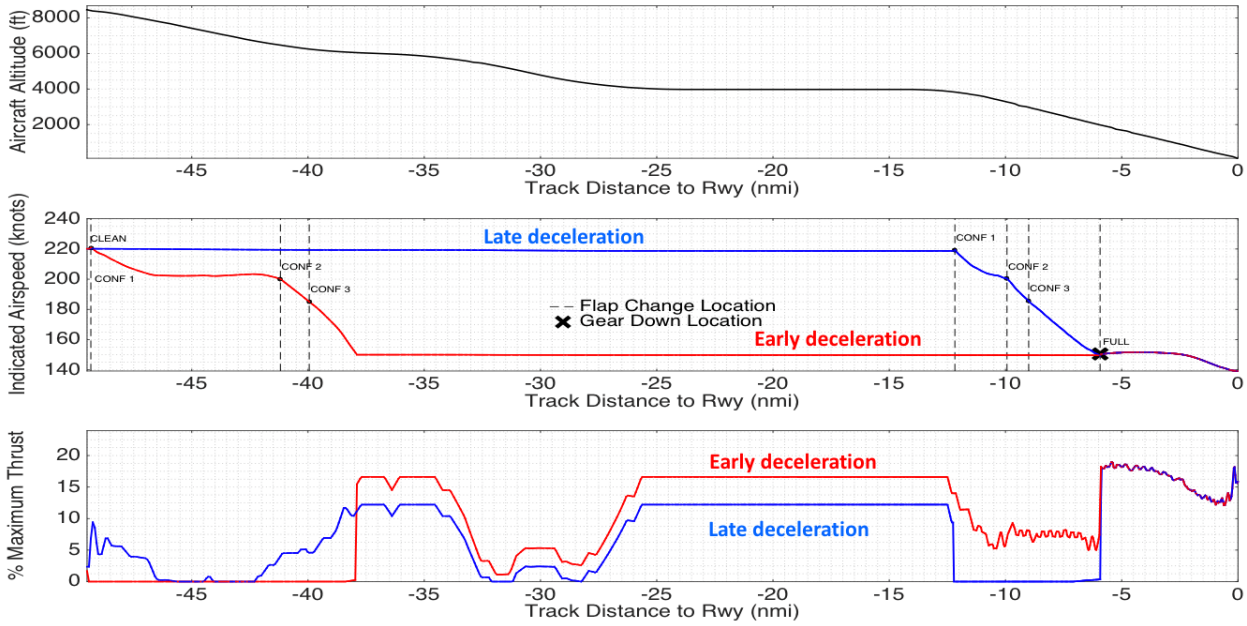

Figure 22. Late (blue) and early (red) deceleration profiles.

The difference in SEL generated by the delayed and earliest deceleration flight profiles is shown in **Error! Reference source not found.**, where red indicates the delayed deceleration approach is louder and blue indicates the early deceleration case is louder. While SEL is decreased to the left and right of the flight track for the delayed deceleration case, the delayed deceleration noise is neutral or slightly higher increased directly underneath the flight track. To clarify the cause of the difference in noise between the two flight profiles, the contributions due to both engine and airframe are also plotted separately in **Error! Reference source not found.**. It is apparent that the increase in thrust throughout much of the earliest deceleration flight profile results in an increase in engine noise at the noise monitors compared to the latest deceleration case. However, the increased aircraft speed for most of the latest deceleration profile results in an increase in airframe noise at the noise monitors compared to the earliest deceleration case. Employing the delayed deceleration approach in this scenario results in an increase in airframe noise that outweighs the decrease engine noise at the noise monitors and underneath much of the flight track.

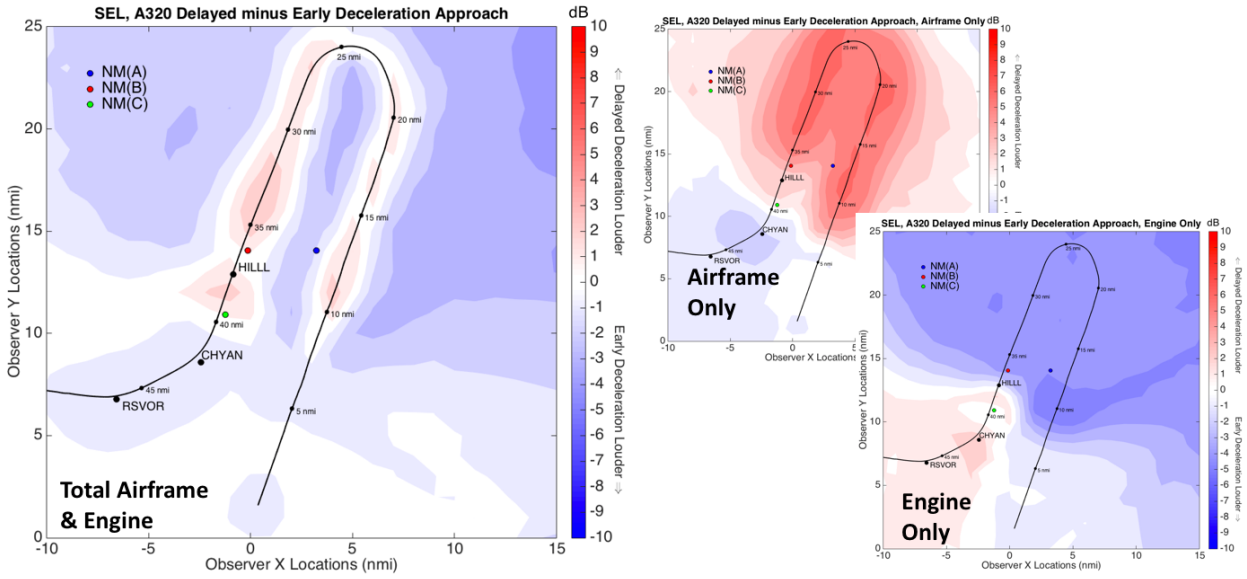

Figure 23. Difference in modeled SEL between late and early deceleration case in terms of total noise (left) and broken down by noise source (right).

Publications

None

Outreach Efforts

None

Awards

None

Student Involvement

Graduate students have been involved in all aspects of the research

Plans for Next Period

This the final report for the Penn State activities.

References

[1] T. G. Reynolds, Y. Rodriguez, M. Mcpartland, and M. Sandberg, "Assessment of Delayed Deceleration Approach Opportunities at US Airports," AIAA Paper No. 2015-2433, June 2015.

[2] E. R. Boeker, E. Dinges, B. He, G. Fleming, C. J. Roof, P. J. Gerbi, A. S. Rapoza, and J. Hemann, "Integrated Noise Model (INM)Version 7.0 Technical Manual," 2008.

[3] Federal Aviation Administration, "The FAR Part 150 Airport Noise Compatibility Planning Program: An Overview." https://www.faa.gov/about/office_org/headquarters_offices/apl/noise_emissions/planning_toolkit/media/II.B.pdf, Last referenced 2/12/2018.
[4] Massachusetts Port Authority, "Boston Logan International Airport: 2014 Environmental Data Report," 2014. http://massportcac.org/wp-content/uploads/2016/09/2014_EDR_Web_Version_file1-compressed.pdf, Last referenced 2/12/2018.
[5] Sourdine II Consortium, "Sourdine II Final Report," 2001. https://trimis.ec.europa.eu/sites/default/files/project/documents/20100310_134424_75167_Sourdine%20II%20Final%20Report.pdf, Last referenced 2/12/2018.
[6] L. V. Lopes and C. Burley, "ANOPP2 User's Manual"," NASA/TM–2016–219342, 2016.
[7] M. Drela, "TASOPT 2.00 Transport Aircraft System OPTimization Technical Description," 2010. http://web.mit.edu/drela/Public/N+3/Final_Report_App.pdf, Last referenced 2/12/2018.
[8] A. Nuic, "User Manual for the Base of Aircraft Data (BADA) - Revision 3.6," 2004. https://www.eurocontrol.int/sites/default/files/library/022_BADA_User_Manual.pdf, Last referenced 2/12/2018.
[9] Airbus Training, "A320 Flight Crew Operating Manual, Operating Limitations," Airbus FCOM 3.01.70.
[10] J. R. Ratley, M. F. Coker, R. P. Craig, J. O. Creighton, and J. M. Eitel, "737-600/700/800/900 Flight Crew Training Manual." The Boeing Company, 2005.
[11] "FAA Advisory Circular 36-1H - Noise Levels for U.S. Certificated and Foreign Aircraft, Appendix 1 (U.S. Certificated Turbojet Powered Airplanes)," 2012.
[12] M. F. Heidmann, "Interim Prediction Method for Fan and Compressor Source Noise," NASA Tech. Memo. X-71763, 1979.
[13] J. W. Hough and D. S. Weir, "Aircraft Noise Prediction Program (ANOPP) Fan Noise Prediction for Small Engines," NASA *Contract. Rep. 198300*, 1996.
[14] K. Kontos, B. Janardan, and P. Gliebe, "Improved NASA-ANOPP Noise Prediction Computer Code for Advanced Subsonic Propulsion Systems Volume 1: ANOPP Evaluation and Fan Noise Model Improvement," NASA *Contract . Rep. 195480*, 1996.
[15] E. Krejsa and J. R. Stone, "Enhanced Fan Noise Modeling for Turbofan Engines," NASA *Contract . Rep. 2014-218421*, 2014.
[16] M. R. Fink, "Airframe Noise Prediction Method," FAA Report RD-77-29, 1977.
[17] Y. Guo, "Aircraft Slat Noise Modeling and Prediction," 16th AIAA/CEAS Aeroacoustics Conf., AIAA Paper No. 2010-3837, June 2010.
[18] Y. Guo, "Aircraft Flap Side Edge Noise Modeling and Prediction," 17th AIAA/CEAS Aeroacoustics Conf., AIAA Paper No. 2011-2731, 2011.
[19] Y. Guo, "Empirical Prediction of Aircraft Landing Gear Noise," NASA *Contract. Rep. 2005-213780*, 2005.
[20] J.-M. Dumont, "Fuel Burn Reduction Potential from Delayed Deceleration Approaches," MS thesis, Department of Aeronautics and Astronautics, Massachusetts Institute of Technology, 2012.